JOC Article

Addition of Organolithium Reagents to Corannulene and Conformational Preferences in 1-Alkyl-1,2-dihydrocorannulenes

Andrzej Sygula,*[,†] Renata Sygula,[†] Frank R. Fronczek,[‡] and Peter W. Rabideau*[,†]

Department of Chemistry and Ames Laboratory, Iowa State University, Ames, Iowa 50011, and Department of Chemistry, Louisiana State University, Baton Rouge, Louisiana 70103

asygula@iastate.edu; rabideau@iastate.edu

Received April 23, 2002

Addition of organolithium reagents to corannulene (**1**) produces 1-R-1,2-dihydrocorannulenes **(2)**, which can be easily converted to 1-R-corannulenes (**3**). Molecular mechanics (MM) calculations predict a slight pseudoequatorial preference for the small substituents in both *exo* and *endo* arrangements of **2**, whereas bulky substituents are expected to favor strongly the *exo*-pseudoaxial location. X-ray diffraction studies show the *exo*-pseudoaxial conformation in the solid state for both *i*-Pr and *t*-Bu-**2**. In solution, a gradual increase in the contribution of pseudoequatorial conformations with decreasing size of the substituent is demonstrated by analysis of the ^3J H−H coupling constants within the reduced ring.

Introduction

The discovery of buckminsterfullerene (C_{60}) has led to considerable interest in the synthesis and study of curved-surface polynuclear aromatic hydrocarbons whose carbon frameworks can be identified on the C_{60} surface ("buckybowls").[1] Corannulene (**1**), a bowl-shaped $C_{20}H_{10}$ hydrocarbon,[2] is the simplest example, and its carbon framework represents the polar cap of buckminsterfullerene. Recent improvements in the synthesis of **1** have allowed for more extensive studies of its chemistry and also preparation of derivatives.[3] For example, syntheses of alkylated corannulenes have been reported, generally through alkylation of halocorannulenes or by incorporation of alkyl groups prior to the final ring closure step that produces curvature.

The addition of alkyllithiums to polycyclic aromatic hydrocarbons (PAHs) represents a well-established methodology for the synthesis of alkylated dihydro-PAHs as well as alkyl-PAHs.[4] An earlier report from Scott's laboratory showed that *tert*-butyllithium adds to corannulene to produce 1-*tert*-butyl-1,2-dihydrocorannulene.[5] Since corannulene is now available on a multigram scale through the simple and inexpensive carbenoid coupling of tetrakis(dibromomethyl)fluoranthenes,[3f] we decided to further explore alkyllithium additions, since they could potentially provide a convenient route for the derivatization of **1**. Herein, we report that this method does indeed provide an efficient route to some 1-alkyl-1,2-dihydrocorannulenes, and also alkylcorannulenes as well. We also provide the results of solid-state X-ray and solution ^{1}H NMR studies that examine the conformational preferences of dihydrocorannulenes. Finally, the results of theoretical studies by both molecular mechanics (MM) and density functional theorem (DFT) calculations are presented and compared with analogous results for other structurally related 1,3-cyclohexadienes, as well as with the experimental data.

Results and Discussion

Addition of Organolithiums to Corannulene. The addition of various alkyllithium reagents to corannulene (**1**) in dry THF at −78 °C results in the development of a deep blue color. However, quenching of the reaction

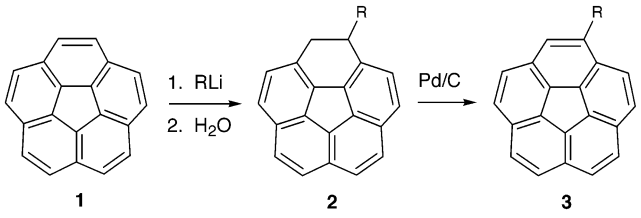

mixture at this temperature only produces starting material. Raising the temperature to 0 °C generally

† Iowa State University.
‡ Louisiana State University.

(1) For the recent reviews, see: (a) Rabideau, P. W.; Sygula, A. *Acc. Chem. Res.* **1996**, *29*, 235. (b) Scott, L. T. *Pure Appl. Chem.* **1996**, *68*, 291. (c) Mehta, G.; Rao, H. S. P. *Tetrahedron* **1998**, *54*, 13325. (d) Scott, L. T.; Bronstein, H. E.; Preda, D. V.; Anselms, R. B. M.; Bratcher, M. S.; Hagen, S. *Pure Appl. Chem.* **1999**, *71*, 209.

(2) (a) Barth, W. E.; Lawton, R. G. *J. Am. Chem. Soc.* **1966**, *88*, 380. (b) Barth, W. E.; Lawton, R. G. *J. Am. Chem. Soc.* **1971**, *93*, 1730.

(3) (a) Scott, L. T.; Cheng, P.-C.; Hashemi, M. M.; Bratcher, M. S.; Meyer, D. T.; Warren, H. B. *J. Am. Chem. Soc.* **1997**, *119*, 10963. (b) Seiders, T. J.; Baldridge, K. K.; Siegel, J. S. *J. Am. Chem. Soc.* **1996**, *118*, 2754. (c) Seiders, T. J.; Baldrige, K. K.; Elliott, E. L.; Grube, G. H.; Siegel, J. S. *J. Am. Chem. Soc.* **1999**, *121*, 7439. (d) Sygula, A.; Rabideau, P. W. *J. Am. Chem. Soc.* **1999**, *121*, 7800. (e) Seiders, T. J.; Elliott, E. L.; Grube, G. H.; Siegel, J. S. *J. Am. Chem. Soc.* **1999**, *121*, 7804. (f) Sygula, A.; Rabideau, P. W. *J. Am. Chem. Soc.* **2000**, *122*, 6323. (g) Seiders, T. J.; Baldridge, K. K.; Grube, G. H.; Siegel, J. S. *J. Am. Chem. Soc.* **2001**, *123*, 517.

(4) Harvey, R. G. *Polycyclic Aromatic Hydrocarbons*; Wiley-VCH: New York, 1997; p 99.

(5) Cheng, P.-C. M.S. Thesis, University of Nevada, Reno, 1992.

10.1021/jo0258498 CCC: $22.00
Published on Web 08/07/2002

produces optimum results for addition, while at higher temperatures other processes occur, resulting in a complicated mixture of products.

Despite several attempts, however, this procedure was not successful for monoalkylation with methyllithium. At 0 °C, even after several hours, no 1-Me-1,2-dihydrocorannulene (**2b**) is formed, and starting material is recovered, while at higher temperatures several overmethylated products are produced. On the other hand, both isopropyl- and *tert*-butyllithium add smoothly to **1** at 0 °C, forming the 1-*i*-Pr-1,2-dihydro-**1** and 1-*t*-Bu-1,2-dihydro-**1** (**2c** and **d**) derivatives which were isolated in good yields and fully characterized by spectroscopic methods as well as by X-ray single-crystal diffraction studies. In an attempt to incorporate less bulky substituents, we turned to trimethylsilymethyllithium and benzyllithium. These organolithium reagents did produce the desired 1-(TMS−CH_2)-1,2-dihydrocorannulene (**2e**) and 1-Bz-1,2-dihydrocorannulene (**2f**), but the additions were sluggish and provided mixtures that included starting material **1**, rearomatized 1-R-corannulenes (**3**), and, in the case of **2e**, also 1,2-dihydrocorannulene (**2a**). Separation of the mixtures proves to be elaborate and time-consuming, and so, this synthetic protocol is not as attractive for the synthesis of 1-R-**2** with less bulky substituents.

1,2-Dihydrocorannulenes may be efficiently converted to corannulenes by dehydrogenation with palladium on activated carbon in refluxing diglyme. Both **2c** and **d** may be converted to *i*-Pr-corannulene (**3c**) and *t*-Bu-corannulene (**3d**), respectively, in high yields, offering an alternative synthetic pathway to these previously reported derivatives. Also, when the mixture of **2f** and 1-benzylcorannulene (**3f**) is refluxed overnight with Pd/C, it cleanly produces 1-benzylcorannulene in an isolated yield of ∼40% for the two steps.

Conformational Preferences in 1-Alkyl-1,2-dihydrocorannulenes. The partially hydrogenated six-membered ring in 1,2-dihydrocorannulene (**2a**) is structurally similar to the central ring of 9,10-dihydrophenanthrene (**4**); the latter system has been widely studied, and its stereochemistry and conformational preferences are well documented in the literature.[6] The reduced rings in both **2a** and **4** adopt nonplanar, semichair conformations of C_1 and C_2 symmetries, respectively. However, the presence of additional aromatic rings in **2a** "clipping" the molecular framework together introduces two novel structural aspects when compared to the case of **4**. First, the partially hydrogenated ring in **2a** is much flatter than that in **4**. The degree of folding can be adequately described by two torsion angles: α1, which describes the torsion of the two formally ethylenic units along the pivotal bond ($C_{2a}-C_{10c}-C_{10b}-C_{10a}$ in **2a** and $C_{8a}-C_{4b}-C_{4a}-C_{10a}$ in **4**), and α2, describing the conformation along the $C_{sp3}-C_{sp3}$ linkage ($C_{10a}-C_1-C_2-C_{2a}$ in **2a** and $C_{8a}-C_9-C_{10}-C_{10a}$ in **4**). An X-ray crystal structure determination of 9,10-dihydrophenanthrene (**4**) shows α1 values in the range 18.9−21.9° and α2 angles in the range 53.4−56.4°.[7] In contrast, our MM2 and

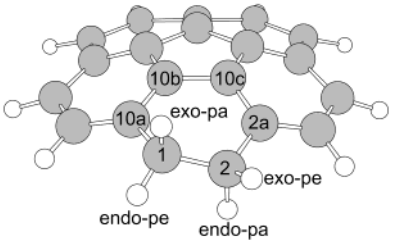

2a

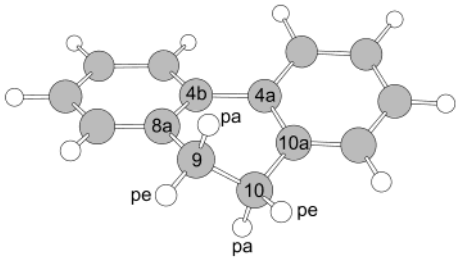

4

Becke3LYP/3-21G calculations predict the partialy reduced ring in 1,2-dihydrocorannulene **2a** to be significantly flatter with α1 and α2 in the range of only 6.0−8.2° and 32.7−33.7°, respectively. Second, the classical *pseudoaxial* (*pa*) versus *pseudoequatorial* (*pe*) competition in **4** becomes more complicated in **2**. Since the surface of the corannulene system is curved, the two *pa* positions in **2a** are no longer equivalent as they are in **4**, and the same holds true for the *pe* positions. Thus, for substituents with local C_3 symmetry, like Me and *t*-Bu, there are four distinct conformers to be considered: (1) *endo-pseudoaxial* (*endo-pa*), (2) *endo-pseudoequatorial* (*endo-pe*), (3) *exo-pseudoaxial* (*exo-pa*), and (4) *exo-psudoequatorial* (*exo-pe*), where *endo* and *exo* are related to concave and convex orientations, respectively.

Table 1 presents the MM2 strain energies of all conformers considered for a series of 1-R-1,2-dihydrocorannulenes, with R = Me (**2b**), *i*-Pr (**2c**), and *t*-Bu (**2d**). For the *i*-Pr derivative **2c**, the number of conformers to be considered is larger, since the substituent can accommodate three different rotameric orientations of the *i*-Pr group for each conformation considered; thus, 12 distinct conformations of **2b** were taken into account.

9-Monosubstituted-dihydrophenanthrenes (**4**) show a strong preference for pseudoaxial substituent location, a result of the severe repulsive interaction of a pseudoequatorial substituent with the peri-hydrogen atom at C_8.[6] Accordingly, MM2 predicts the trend showing the pseudoaxial conformers to be more stable by 0.9, 2.5, and 6.2 kcal/mol for 9-Me, 9-*i*-Pr, and 9-*t*-Bu-**4**, respectively.

The results for the dihydrocorannulenes (Table 1) reveal that this system behaves quite differently than **4**. For **2b**, all four conformations exhibit similar strain energies with a slight preference for the pseudoequatorial orientation of the methyl group by ∼0.4 kcal/mol in both *exo* and *endo* arrangements. In contrast, the *t*-Bu group prefers a pseudoaxial orientation in the *exo* conformer by 2.0 kcal/mol over the energy of the pseudoequatorial one, while the energies of the pseudoaxial and pseudoequatorial conformers in the *endo* arrangement are virtually the same. In the case of *exo*-**2d**, this resembles, to some extent, the preferences in **4**, although the relative

(6) For a review, see: Rabideau, P. W.; Sygula, A. In *The Conformational Analysis of Cyclohexenes, Cyclohexadienes, and related Hydroaromatic Compounds*; Rabideau, P. W., Ed.; VCH Publishers: New York, 1989; Chapter 3, p 65.

(7) Cosmo, R.; Hambley, T. W.; Sternhell, S. *J. Org. Chem.* **1987**, *52*, 3119.

TABLE 1. MM2 Strain Energies (kcal/mol) for 1-Alkyl-1,2-dihydrocorannulenes 2b−d

	endo-pa	*endo-pe*	*exo-pa*	*exo-pe*
1-Me (**2b**)	19.13	18.74	19.18	18.74
1-*i*-Pr (**2c**)	25.04	22.58	22.76	21.87
	22.13	24.25	22.47	23.93
	23.33	23.29	22.01	23.56
1-*t*-Bu (**2d**)	26.91	27.15	24.31	26.28

stabilization of the pseudoaxial conformer in **2d** is more modest. The picture for the *i*-Pr derivative **2c** is somewhat obscured by the large number of rotamers considered. However, when the lowest energy conformers are considered, the pseudoaxial and pseudoequatorial conformers in the *exo* arrangement are virtually identical in energy, while, in the *endo* arrangement, the pseudoaxial position is slightly preferred over the pseudoequatorial one by ~0.4 kcal/mol.

The pseudoaxial versus pseudoequatorial preference of alkyl groups in **2** may be rationalized as follows. Geometry constraints within the corannulene ring system force the reduced ring to be significantly flattened relative to **4** (see earlier). The stereochemical consequence of this flattening is that the distance between the pseudoequatorial substituent at C_1 and the peri-hydrogen atom at C_{10} is significantly larger for **2** than the analogous distance in **4**. This, of course, greatly reduces the repulsions that are responsible for the strong pseudoaxial preference in **4**. For small substituents, like Me in **2b**, the repulsion vanishes almost completely and the 1,3-diaxial interactions become overriding, causing the pseudoequatorial conformer to be more stable, analogous to the 1,3-cyclohexadiene system.[6] However, for bulky substituents, like *t*-Bu in **2d**, the peri-repulsions become important again, destabilizing the pseudoequatorial position relative to the pseudoaxial conformation. However, the preference for the pseudoaxial conformation in **2d** is much more modest than that in 9-*t*-Bu-**4** (6.2 kcal/mol) because of the reduction of peri-repulsions caused by flattening of the ring in **2** relative to **4**.

Exo versus Endo Preferences. Table 1 shows no apparent *exo*/*endo* preference for the methyl group in **2b**, since the MM2 strain energies are virtually identical for *exo*/*endo* pairs of both pseudoaxial and pseudoequatorial conformers. In contrast, MM2 provides strong evidence for *exo* preference with bulky substituents, as demonstrated in the case of **2d**. Both pseudoaxial and pseudoequatorial conformers of *endo*-**2d** have higher strain energies than that of the most stable conformer, *exo*-pseudoaxial-**2d**, by 2.6−2.8 kcal/mol. Even the nonpreferred, *exo*-pseudoequatorial conformer is lower in energy than either *endo*-conformer of **2d**.

The *i*-Pr group in **2c** shows a slight preference for the *exo* position. With the lowest energy rotamers considered, both *exo*-**2c** conformers are more stable than their *endo* counterparts, but only by 0.1−0.5 kcal/mol. However, the preference is more pronounced when the energies are averaged over three rotamers (unweighted averages) for each conformation, resulting in *exo*-pseudoaxial-**2c** as the best conformation with average energies of 0.7, 1.0, and 1.1 kcal/mol lower than those of the *exo*-pseudoequatorial, *endo*-pseudoequatorial, and *endo*-pseudoaxial conformers, respectively. Nonetheless, MM2 calculations suggest that the *exo* conformations are only very slightly preferred over *endo* in **2c**.

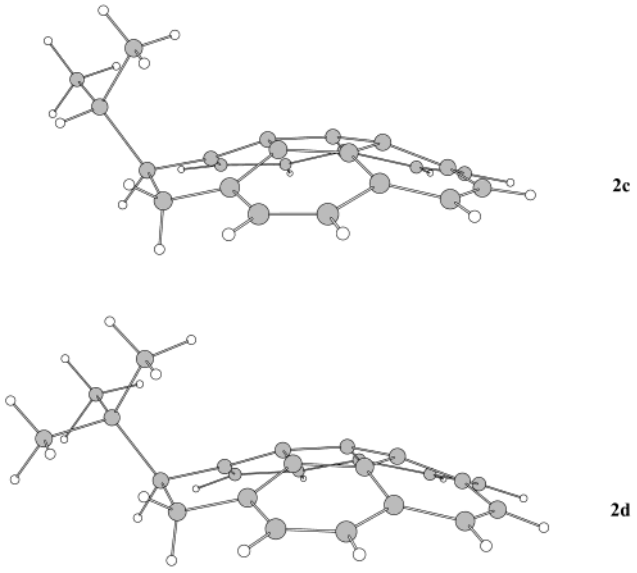

FIGURE 1. X-ray crystal structures of **2c** and **d**.

A rationalization for the *exo* preference of bulky substituents may be drawn from a closer inspection of the structures of *endo*-**2d** as generated by MM2. Repulsive interactions of the *t*-Bu group with the hydrogen atom at C_{10} (peri-interaction) are responsible for destabilization of both the *endo*-pseudoequatorial and *endo*-pseudoaxial conformers, and this is not surprising in the case of the pseudoequatorial conformer (see earlier). However, the pseudoaxial *t*-Bu in *endo*-**2d** also suffers from a repulsion with the peri-hydrogen atom, and to minimize this repulsion, the reduced ring becomes more folded. The MM2 calculated α1 and α2 torsion angles for *endo*-pseudoaxial-**2d** are 10 and 45°, significantly larger than the values in the *exo*-pseudoaxial conformer (9 and 34°, respectively). Moreover, the latter values are very close to those for unsubstituted **2a**, showing that there is no significant strain introduced by *t*-Bu located in the *exo*-pseudoaxial position.

Crystal Structure Determination of 2c and d. Crystals of **2c** and **d**, obtained by slow evaporation of methanol and chloroform solutions, respectively, have been subjected to X-ray diffraction studies. These dihydro derivatives of corannulene retain preference for the bowl-shaped conformation, similar to the case of parent **1**. In the solid state, the average distance of the eight sp^2 hybridized rim carbon atoms from the plane defined by the central five-membered ring is 0.86 Å for both **2c** and **d**, as compared to 0.89 Å for **1**.[8] Both *i*-Pr and *t*-Bu groups adopt *exo*-pseudoaxial positions in the crystal (Figure 1). This conformer is predicted by MM2 to be the most stable for **2d** by at least 2 kcal/mol (Table 1). On the other hand, the MM2 calculation for the rotamer of *exo-pa*-**2c** found in the crystal showed a strain energy of 22.0 kcal/mol, and this represents the second lowest energy of all 12 conformers of **2c**, only 0.1 kcal/mol higher than that of the lowest energy rotamer of *exo-pe*-**2c** (21.9 kcal/mol, Table 1). Reoptimization of both conformers at the

(8) Hanson, J. C.; Nordman, C. E. *Acta Crystallogr., Sect. B* **1976**, *32*, 1147.

TABLE 2. Selected Torsion Angles (deg) for the Reduced Ring in 2c and d, as Found in the Crystal and Calculated by MM2 and B3LYP

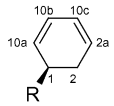

	R = *i*-Pr			R = *t*-Bu		
torsion angle	X-ray[a]	MM2	B3LYP	X-ray[a]	MM2	B3LYP
$C_{2a}-C_{10c}-C_{10b}-C_{10a}$ (α1)	5.2 (1.7)	7.5	4.8	4.0 (0.4)	8.7	5.2
$C_{10a}-C_1-C_2-C_{2a}$ (α2)	28.2 (1.3)	29.8	25.3	24.8 (0.4)	33.6	29.0
$C_1-C_{10a}-C_{10b}-C_{10c}$	19.5 (1.5)	17.4	19.4	18.3 (0.4)	18.0	20.6
$C_2-C_{2a}-C_{10c}-C_{10b}$	−13.1 (1.5)	−12.0	−12.4	−10.4 (0.4)	−12.0	−11.9
$C_\alpha-C_1-C_2-C_{2a}$	−102.4 (1.1)	−97.3	−100.9	−104.6 (0.3)	−94.4	−97.8
$C_\alpha-C_1-C_{10a}-C_{10b}$	95.6 (1.0)	93.0	93.0	99.1 (0.3)	92.4	92.0
$C_\beta-C_\alpha-C_1-C_2$	62.8 (1.1)	64.3	64.7			
$C_{\beta'}-C_\alpha-C_1-C_2$	−174.5 (0.9)	−171.3	−170.5			

[a] Standard deviation in parentheses.

Becke3LYP/3-21G level, followed by single point calculations at the Becke3LYP/6-31G** level, shows that at this level of theory the *exo-pa* conformer is very slightly favored by ~0.1 kcal/mol. The small difference in stabilities prohibits any conclusions as to the origin of the *exo-pa* preference in the crystal, which may be the result of crystal packing forces or may represent a genuine preference for that geometry.

The reduced rings in both derivatives exhibit a significant degree of twisting along the C_1-C_2 bond. Table 2 compares the conformations of the reduced rings in the solid state with those predicted for the isolated molecules by MM2 and Becke3LYP/3-21G calculations.

The agreement between the X-ray results and both theoretical models is very good, proving that packing forces do not significantly influence the conformational preferences of the isolated molecules. The Becke3/LYP torsional angles are slightly closer to the experimental values than those from MM2 calculations. The only notable difference between the models and experiment is that the reduced ring for **2d** in the solid state is slightly flatter than that for **2c** (Table 2). Considering the size of the substituents, the opposite trend might be expected on the basis of chemical intuition, and this latter expectation is supported by both MM2 and Becke3LYP/3-21G calculations which predict slightly larger torsion angles in the ring of isolated **2d**. However, comparison of the calculated torsion angles within the reduced rings in **2a**, **c**, and **d** shows that introduction of a bulky substituent does not change the degree of folding significantly, suggesting no strong steric hindrance of the substituents in their lowest energy conformations. Accordingly, the potential energy surfaces, as functions of the angles α1 and α2, are very flat, so even very subtle effects may change the degree of folding to some extent. With this in mind, we conclude that agreement between MM2 predictions and X-ray structures is excellent for **2c** and at least good for **2d**.

Dynamic Processes in 1-R-1,2-Dihydrocorannulenes. While crystal structure determinations usually show only single conformations that are of lowest energy with respect to both intra- and intermolecular interactions, fast interconversion in solution or in gas phase produces a statistical distribution of conformers related to the differences in their relative stabilities.

In 1-R-**2**, there are three dynamic processes to be considered: (a) bowl-to-bowl inversion of the entire dihydrocorannulene moiety interconverting *exo* and *endo* conformers, (b) ring inversion of the 1,3-cyclohexadiene system, which equilibrates pseudoaxial and pseudoequatorial conformers within both the *exo* and *endo* arrangements, and (c) rotation of the substituent around the $C_\alpha-C_1$ bond, which equilibrates the three rotamers within each *endo-exo*/*pa-pe* combination.

All of the dynamic processes discussed earlier are believed to be low energy interconversions. The bowl-to-bowl inversion for corannulene derivatives has been found to be fast on the NMR time scale with barriers of only 10−12 kcal/mol.[1,3g] Dynamic NMR measurements estimate an even lower barrier for 1,2-dihydrocorannulene **2a** (8.5 kcal/mol).[9] Theoretical calculations at the ab initio and local density functional theory (LDF) level have also been reported, providing an estimation of the inversion barriers in **2a** in the range of 7−11 kcal/mol.[9,10]

The "1,3-cyclohexadiene-like" ring inversion is also a low energy process. Our calculations at both MM2 and ab inito levels provide barriers for the inversion in the range of 1.5 kcal/mol, which is even lower than the analogous barriers in 1,3-cyclohexadienes.

Finally, the rotation of the substituent along the pivotal $C_\alpha-C_1$ bond is also a fast process, as suggested by the MM2 calculated energy profile for *i*-Pr group rotation in *exo-pa*-**2c** that shows barriers in the range 3.0−3.5 kcal/mol. Hence, all of the dynamic processes in **2** are fast, at least on the NMR time scale, and its properties will be the result of an equilibrated distribution of conformers in solution and in gas phase.

^{1}H NMR Solution Studies. We have examined the spectra of several dihydrocorannulenes in an attempt to learn something about the conformational preferences in solution. The hydrogen atom at C_1 is coupled by vicinal coupling with two hydrogens at C_2 ($^3J_{cis}$ and $^3J_{trans}$), and these coupling constants should be sensitive to the conformation of the ring and to the location of the substituent. Examination of the MM2 models with ap-

(9) Borchardt, A.; Fuchicello, A.; Kilway, K. V.; Baldridge, K. K.; Siegel, J. S. *J. Am. Chem. Soc.* **1992**, *114*, 1921.
(10) Sygula, A.; Rabideau, P. W. *Chem. Commun.* **1994**, 1497.

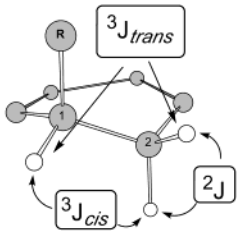

plication of the Karplus relationship[11] reveals that although the $^3J_{cis}$ coupling constant is not very sensitive to conformational changes (with values in the range 5−9 Hz for all conformers considered), $^3J_{trans}$ changes dramatically when going from a pseudoequatorial to pseudoaxial substituent location (from 11 to 1 Hz). Thus, this latter coupling constant may be used for an estimation of the conformational preferences in solution.

The *t*-Bu derivative **2d** is considered first, since it represents the simplest case; that is, a strong preference is predicted for a single conformation corresponding to that found in the solid state. The alicyclic region of the ^{1}H NMR spectrum of **2d** consists of three doublets of doublets at 3.70 (A), 3.08 (B), and 2.73 (C) ppm. Protons A and C are coupled by −18.9 Hz (geminal ^2J coupling), and proton B is coupled to A by 1.6 Hz and to C by 8.7 Hz, which represents ^3J vicinal coupling. Comparison of the vicinal coupling constants with the theoretical expectations for *endo-pa*-**2d** strongly suggests the former to be $^3J_{trans}$ and the latter $^3J_{cis}$. This is further supported by a NOESY experiment which shows a cross-peak of the *t*-Bu protons with the proton at 3.70 ppm but no observable cross-peak with the proton at 2.73 ppm. The theoretically calculated vicinal coupling constants for *exo-pa*-**2d** are in good agreement with the measured values.

Similar analysis of the *i*-Pr derivative (**2c**) shows that the protons with chemical shifts of 3.42 and 3.02 ppm are coupled by geminal ^2J coupling constant of −17.7 Hz and to the proton at C_1 (3.34 ppm) by ^3J coupling constants of 4.8 and 8.7 Hz, respectively. The NOESY experiment proves that the proton at 3.42 ppm is *cis* to the *i*-Pr group.[12] Thus, the larger coupling constant is assigned as $^3J_{cis}$, and the smaller, as $^3J_{trans}$. While the former is basically identical with the analogous coupling in **2d**, $^3J_{trans}$ is significantly higher. This is an obvious indication of the significant presence of the pseudoequatorial conformers for **2c** in solution. Indeed, if one assumes a 50:50 distribution of *pa*/*pe* conformers, the expected $^3J_{trans}$ would be ∼5.5 Hz. A greater population of pseudoequatorial conformers[12] is in accord with the modeling studies that predict the lowest energy *exo-pe* and *exo-pa* conformers to be of virtually the same energy.

The alicyclic protons appear in the ^{1}H NMR spectrum of 1-(TMS−CH_2)-1,2-dihydrocorannulene (**2e**) at 3.74 ppm (multiplet, H at C_1), 3.35 ppm (dd, H_{trans} at C_2), and 3.01 ppm (dd, H_{cis} at C_2). Analysis of this part of the spectrum reveals a geminal ^2J coupling constant of −17.1 Hz and two nearly identical ^3J couplings of 7.5 Hz each. The high value of $^3J_{trans}$ is strong evidence that the contribution of pseudoequatorial conformations in the overall distribution of conformers in **2e** is even higher than that in **2c**.

Analysis of the alicyclic region in the benzyl derivative **2f** is further complicated by the two benzylic protons which overlap to some extent with the signals from the protons at C_2. However, the 500 MHz spectrum allows resolution of the signals, revealing a 3.71 ppm multiplet for the proton at C_1 and four doublets of doublets at 3.52 (A), 3.09 (B), 3.01 (C), and 2.97 (D) ppm. There are two geminal couplings of −13.6 (A−C) and −17.3 Hz (B−D), and by analogy with the previous derivatives, the latter pair of protons are assigned as the alicyclic C_2 protons. This assignment is further supported by the value of the $^2J_{A-C}$ coupling (−13.6 Hz), which is close to the coupling within the methyl group in toluene (−14.5 Hz).[13] Protons B and D are coupled to the proton at C_1 by 6.2 and 7.8 Hz, respectively, and these numbers are very close to the ones predicted for $^3J_{cis}$ and $^3J_{trans}$ in **2b**. However, we are not able to distinguish which ^3J coupling in **2f** represents the *cis* or *trans* relationship. In any case, the contribution of the pseudoequatorial conformations in solutions of **2f** is substantial.

A comparison of the $^3J_{trans}$ coupling constants measured for **2d**, **c**, **e**, and **f** shows increasing values corresponding to a decrease in substituent size. This phenomenon indicates the increasing contribution of the pseudoequatorial conformations to the overall population of the species in solution and, therefore, strongly supports the theoretical predictions for *pa*/*pe* preferences in the system.

Experimental Section

General Procedure for the Addition of Alkyllithiums to Corannulene. A large excess (usually 4−5 equiv) of the appropriate organolithium was added under nitrogen to 20 mg (0.08 mmol) of corannulene dissolved in 3−4 mL of dry THF at −78 °C. The stirred mixture was warmed to 0 °C, and the reaction progress was monitored by GC. The reaction was quenched with aqueous ammonium chloride, and the reaction mixture was extracted with methylene chloride, dried over magnesium sulfate, filtered, and evaporated. The crude mixture was analyzed by GC and GC/MS.

Isopropyllithium. After 30 min at 0 °C, the crude mixture showed 95% of 1-*i*-Pr-1,2-dihydrocorannulene (**2c**) with traces of **1** and *i*-Pr-**1**. Chromatography on a short pad of silica gel with cyclohexane as eluent and subsequent recrystallization from methanol gave **2c** as a pale yellow solid, mp 99−100 °C. ^{1}H NMR (THF-d_8) 1.09 (3H, d, J = 6.9 Hz), 1.23 (3H, d, J = 6.8 Hz), 2.47 (1H, m), 2.99−3.06 (1H, m), 3.33−3.44 (2H, m), 7.20 (1H, d, J = 8.4 Hz), 7.28 (1H, d, J = 8.3 Hz), 7.59−7.70 (6H, m); ^{13}C NMR (THF-d_8) 19.5, 20.4, 31.4, 35.1, 47.0, 126.9, 127.2, 127.6, 127.7, 127.8, 128.2, 128.6, 128.8, 130.9, 131.5, 131.6, 134.5, 134.7, 136.8, 137.2, 138.9, 139.0; MS (*m*/*e*, rel intensity) 294 (26), 251 (100), 249 (44). HRMS calcd for $C_{23}H_{18}$, 294.1408; found, 294.1401. Anal. Calcd for $C_{23}H_{18}$: C, 93.86; H, 6.16. Found: C, 93.57; H, 5.88.

***tert*-Butyllithium.** After 1 h, the reaction mixture showed 86% of 1-*t*-Bu-1,2-dihydrocorannulene (**2d**), 7% of **1**, and 5% of 1-*t*-Bu-corannulene. Recrystallization twice from methanol provided pure **2d**.[5]

Trimethylsilylmethyllithium. After 1.5 h, the reaction mixture showed 49% of 1-trimethylsilyl-1,2-dihydrocorannulene (**2e**), 21% of **1**, 19% of 1-trimethylsilylcorannulene, and

(11) (a) Karplus, M. *J. Am. Chem. Soc.* **1963**, *85*, 2870. (b) Bothner-By, A. B. *Adv. Magn. Res.* **1965**, *1*, 195.

(12) Significant cross-peaks of the 3.42 ppm proton with both diastereotopic methyl groups are observed. A relatively small cross-peak between one of the methyl groups and the other proton at C2 (3.02 ppm) is also found, suggesting some contribution from the pseudoequatorial conformations.

(13) Barfield, M.; Grant, D. M. *J. Am. Chem. Soc.* **1963**, *85*, 1899.

9% of **2a**. However, separation of **2e** could not be achieved by chromatography, and the mixture was analyzed by ^{1}H NMR directly.

Benzyllithium. After 1.5 h, the mixture showed 36% of 1-benzyl-1,2-dihydrocorannulene (**2f**), 49% of **1**, and 14% of 1-benzylcorannulene (**3f**). Although **1** could be separated from the mixture by column chromatography (silica gel, cyclohexane), **2f** and the rearomatized product could not be separated, and NMR analysis was performed on the mixture.

Methyllithium. The above procedure failed with methyllithium. At 0 °C, there was no addition product formed after 3 h of stirring, and overmethylated products were produced at higher temperatures. An attempt at addition at 0 °C with TMEDA also failed, resulting mainly in the recovery of starting material together with two monomethylated products formed in small amounts (below 10% total) and some rearomatized methylcorannulene.

Dehydrogenation of Dihydrocorannulenes. Dihydrocorannulenes were refluxed in diglyme with ~10 mg of 5% Pd on activated carbon. The reaction mixture was then cooled, the solvent was removed under reduced pressure, and the resulting solid was filtered through a short pad of silica gel with benzene. Evaporation of the solvent provided crude 1-alkylcorannulenes with no starting material detectable. 1-Isopropylcorannulene (**3c**) and 1-*tert*-butylcorannulene (**3d**) were obtained by the above procedure with nearly quantitative yields and their identities confirmed by a comparison of the NMR spectra with the published data.[5,14]

1-Benzylcorannulene (3f). Obtained in ~40% yield of the two steps (from **1**). White needles (from methanol). M.p. 153 °C. ^{1}H NMR ($CDCl_3$, 400 MHz) 4.53 (s, 2H), 7.21−7.26 (m, 1H), 7.30−7.37 (m, 4H), 7.57 (s, 1H), 7.72 (d, 1H, J = 8.9 Hz), 7.76−7.81 (m, 6H), 7.87 (d, 1H, J = 8.7 Hz). ^{13}C NMR ($CDCl_3$, 100.6 MHz) 39.2, 125.1, 126.3, 126.5, 126.8, 126.9, 127.1, 128.6, 129.0, 130.4, 130.6, 130.9, 131.1, 135.0, 135.6, 135.8, 135.9, 136.0, 139.6, 140.9. MS (*m*/*e*, rel intensity) 341 (23), 340 (75), 339 (34), 337 (24), 264 (21), 263 (100), 261 (20). HRMS calcd for $C_{27}H_{16}$, 340.1252; found, 340.1259.

Computational Details. Molecular mechanics calculations were performed by the Allinger MM2 method[15] incorporated into the Chem3D program package.[16] DFT calculations were carried out at the hybrid B3LYP level[17] with 3-21G[18a] and 6-31G(d,p)[18b] basis sets employed for geometry optimization and single point calculations, respectively, using the Gaussian92/DFT program package.[19]

Acknowledgment. This work was supported by the Ames Laboratory, which is operated for the U.S. Department of Energy by Iowa State University under Contract No. W-7405-Eng-82.

Supporting Information Available: CIF files for **2c** and **d**. B3LYP geometries and energies for **2a**, *exo-pa*-**2c**, *exo-pe*-**2c**, and *exo-pa*-**2d**. This material is available free of charge via the Internet at http://pubs.acs.org.

JO0258498

(14) Ayalon, A.; Sygula, A.; Cheng, P.-C.; Rabinovitz, M.; Rabideau, P. W.; Scott, L. T. *Science* **1994**, *265*, 1065.

(15) Burket, U.; Allinger, N. L. *Molecular Mechanics*; ACS Monograph 177; American Chemical Society: Washington, DC, 1982.

(16) *CS Chem3D Pro*, version 5.0, CambridgeSoft: Cambridge, MA, 1999.

(17) (a) Becke, A. D. *J. Chem. Phys.* **1993**, *98*, 1372. (b) Becke, A. D. *J. Chem. Phys.* **1993**, *98*, 5648. (c) Lee, C.; Yang, W.; Paar, R. G. *Phys. Rev. B: Condens. Matter* **1988**, *37*, 785.

(18) (a) Binkley, J. S.; Pople, J. A.; Hehre, W. J. *J. Am. Chem. Soc.* **1980**, *102*, 939. (b) Krishnan, R.; Binkley, J. S.; Seeger, R.; Pople, J. A. *J. Chem. Phys.* **1980**, *72*, 650.

(19) Frisch, M. J.; Trucks, G. W.; Head-Gorden, M.; Gill, P. M. W.; Wong, M. W.; Foresman, J. B.; Johnson, B. G.; Schlegel, H. B.; Robb, M. A.; Replogle, E. S.; Gomperts, R.; Andres, J. L.; Rahavachari, K.; Binkley, J. S.; Gonzalez, C.; Martin, R. L.; Fox, D. J.; Defrees, D. J.; Baker, J.; Stewart, J. J. P.; Pople, J. A. *Gaussian 92*; Gaussian, Inc.: Pittsburgh, PA, 1992.